The Journal of Experimental Biology 216, 470-479

doi:10.1242/jeb.073742

RESEARCH ARTICLE

Adaptation to different salinities exposes functional specialization in the intestine of the sea bream (*Sparus aurata* L.)

Sílvia F. Gregório[1], Edison S. M. Carvalho[1], Sandra Encarnação[1], Jonathan M. Wilson[2], Deborah M. Power[1], Adelino V. M. Canário[1] and Juan Fuentes[1,*]

[1]Centre of Marine Sciences (CCMar), CIMAR – Laboratório Associado, Universidade do Algarve, Campus de Gambelas, 8005-139 Faro, Portugal and [2]Laboratório de Ecofisiologia, Centro Interdiscplinar de Investigação Marinha e Ambiental (CIIMAR), Universidade do Porto, Rua dos Bragas 289, 4050-123 Porto, Portugal

*Author for correspondence (jfuentes@ualg.pt)

SUMMARY

The processing of intestinal fluid, in addition to a high drinking rate, is essential for osmoregulation in marine fish. This study analyzed the long-term response of the sea bream (*Sparus aurata* L.) to relevant changes of external salinity (12, 35 and 55 p.p.t.), focusing on the anterior intestine and in the less-often studied rectum. Intestinal water absorption, epithelial HCO_3^- secretion and gene expression of the main molecular mechanisms (SLC26a6, SLC26a3, SLC4a4, atp6v1b, CFTR, NKCC1 and NKCC2) involved in Cl^- and HCO_3^- movements were examined. The anion transporters *SLC26a6* and *SLC26a3* are expressed severalfold higher in the anterior intestine, while the expression of *Atp6v1b* (V-type H^+-ATPase β-subunit) is severalfold higher in the rectum. Prolonged exposure to altered external salinity was without effect on water absorption but was associated with concomitant changes in intestinal fluid content, epithelial HCO_3^- secretion and salinity-dependent expression of *SLC26a6*, *SLC26a3* and *SLC4a4* in the anterior intestine. However, the most striking response to external salinity was obtained in the rectum, where a 4- to 5-fold increase in water absorption was paralleled by a 2- to 3-fold increase in HCO_3^- secretion in response to a salinity of 55 p.p.t. In addition, the rectum of high salinity-acclimated fish shows a sustained (and enhanced) secretory current (I_{sc}), identified *in vitro* in Ussing chambers and confirmed by the higher expression of *CFTR* and *NKCC1* and by immunohistochemical protein localization. Taken together, the present results suggest a functional anterior–posterior specialization with regard to intestinal fluid processing and subsequently to salinity adaptation of the sea bream. The rectum becomes more active at higher salinities and functions as the final controller of intestinal function in osmoregulation.

Key words: marine fish, salinity, intestine, ion transport, HCO_3^- secretion, water absorption.

Received 12 April 2012; Accepted 20 September 2012

INTRODUCTION

Marine fish sustain an ionic disequilibrium with the surrounding water and keep their plasma at around 300 mOsm kg^{-1}. The key organs that sustain this ion asymmetry are the gills and the intestine, while the kidneys play a minor role. The gills have been the focus of several studies because of their central importance in the removal of excess salts (Evans et al., 2005). Water ingestion in the form of drinking is known to be a prevailing mechanism in seawater fish when compared with their freshwater counterparts and by itself provides the raw material for potential water absorption (Fuentes and Eddy, 1997b). However, the ingested fluid needs to be processed to allow for net water absorption in the intestine. The primary step of net ion assimilation driven by NaCl takes place in the esophagus and facilitates water absorption in the intestine (Hirano and Mayer-Gostan, 1976; Parmelee and Renfro, 1983).

In addition to the salinity- and endocrine-regulated drinking process (Fuentes and Eddy, 1997a; Fuentes and Eddy, 1997c), the subsequent net absorption of fluid is essential for maintenance of the osmoregulatory process. Effects of salinity have been shown in eels, where the intestinal water absorption in seawater animals is far higher than in freshwater animals (Aoki et al., 2003; Kim et al., 2008; Skadhauge, 1969). At the molecular level, the water absorption mechanisms in the intestine of marine fish are driven by NaCl *via* an apical $Na^+/K^+/2Cl^-$ co-transporter (Musch et al., 1982) associated with a basolateral Na^+/K^+-ATPase, which has higher activity after adaptation of rainbow trout to seawater (Fuentes et al., 1997). However, there is also growing evidence for the contribution of the apical anion exchangers to Cl^- and water absorption in the intestine of marine fish (Grosell, 2006; Grosell, 2011; Grosell et al., 2005).

An additional aspect to fluid absorption in marine fish is the formation of luminal carbonate aggregates in the intestine, which has been proposed to be central to the preservation of body fluid homeostasis (Grosell, 2006; Grosell and Genz, 2006; Kurita et al., 2008; Wilson et al., 2002). The link between calcium precipitation, luminal fluid alkalinization and absorption has been further experimentally characterized in European flounder (*Platichthys flesus*) *in vivo* (Cooper et al., 2010; Whittamore et al., 2010).

Carbonate aggregate formation is driven by two factors: high divalent ion concentration and the required alkalinization of the intestinal fluid to precipitate calcium carbonate. The first premise is met by the high calcium concentration of seawater, which reaches the intestine in a concentration range that varies between 3 and 15 mmol l^{-1} depending on the species (Fuentes et al., 2006; Genz et al., 2011; Wilson et al., 2002). The alkaline condition is driven by epithelial HCO_3^- secretion (Grosell, 2006), which results in elevated concentrations of HCO_3^- in the intestinal fluid that in turn favors

chemical precipitations of divalent cations in the form of carbonate aggregates. The trapping of divalent cations makes them unavailable for absorption and lowers intestinal fluid osmolality by 70–100 mOsm kg^{-1}, thus enhancing water availability for net absorption (Grosell et al., 2009b; Wilson et al., 2002).

The mechanisms that drive luminal secretion of HCO_3^- in the epithelial cell are complex and still under examination. The presence of a basolateral Na^+/HCO_3^- co-transporter (NBCe1, SLC4a4) in the Gulf toadfish (*Opsanus beta*) (Taylor et al., 2010) and mefugu (*Takifugu obscurus*) (Kurita et al., 2008) suggests a transcellular route for apical HCO_3^- secretion. However, in the absence of basolateral HCO_3^- a varying amount of alkaline secretion still takes place (Faggio et al., 2011; Fuentes et al., 2010b; Grosell et al., 2009a; Guffey et al., 2011), which originates from hydration of the CO_2 in the intestinal epithelial cell in a process catalyzed by carbonic anhydrase (Grosell et al., 2009a). On the apical side of the epithelial cell, the presence of SLC26a6 (Cl^-/HCO_3^- anion exchanger) has also been established (Grosell et al., 2009b; Kurita et al., 2008). In addition, the presence of an apical bafilomycin-sensitive vacuolar proton pump has been proposed to act as an enhancer of the apical HCO_3^- secretion (Guffey et al., 2011).

The anterior intestine has been the model of choice for studying HCO_3^- secretion in marine fish intestine because of its luminal Cl^- dependence, and also because the anterior intestine shows the highest specific rate of Cl^- (and likely water) absorption (Grosell, 2006). However, as shown for the European flounder (*Platichthys flesus*), HCO_3^- secretion takes place in all regions of the intestinal canal (Wilson et al., 2002), and recent studies in eel have highlighted the relative importance of the rectum in the osmoregulation of marine fish (Aoki et al., 2003; Kim et al., 2008).

The objective of the present study was to expose the main changes induced by salinity adaptation in the anterior intestine and the rectum of the sea bream (*Sparus auratus*), a euryhaline species with the ability to adapt to large changes in environmental salinity (Laiz-Carrion et al., 2005), although not to freshwater (Fuentes et al., 2010a). In order to elucidate the salinity-dependent changes in the intestine of the sea bream, the study focused on: (1) the molecular characterization of the main mechanisms involved in the HCO_3^- secretion route (mediated by SLC26a6, SLC26a3, SLC4a4 and Atp6v1b) and the fluid absorptive/secretory intestinal routes related to Cl^- movement (mediated mainly by NKCC1, NKCC2 and CFTR); and (2) the related water absorption and HCO_3^- secretion *in vitro*.

MATERIALS AND METHODS

Animals and experimental conditions

Sea bream (*S. aurata*) juveniles were obtained from commercial sources (CUPIMAR SA, Cadiz, Spain). Fish were quarantined for 60 days in Ramalhete Marine Station (University of Algarve, Faro, Portugal) in 1000 l tanks with running seawater at a density of <5 kg m^{-3} and fed twice daily to a final 2% of body mass (M_b), with a commercial sea bream diet (Sorgal, Ovar, Portugal). In all instances, feeding was withheld for 36 h before sample collection to ensure the absence of undigested food in the intestine.

For salinity adaptation, 90 juvenile sea bream (20–30 g M_b) were separated into three equal groups and transferred from water at 35 p.p.t. salinity to 250 l tanks in three separate closed water circuits with biological filtering with final salinities of 12, 35 or 55 p.p.t., temperature of 21°C and a 14 h:10 h light:dark photoperiod. Increases in salinity were achieved by adding the required amount of Instant Ocean sea salts to control seawater (35 p.p.t.), and decreases in salinity were achieved by dilution of control water with dechlorinated tap water. No mortalities were registered during the experimental period.

All animal manipulations were carried out in compliance with the Guidelines of the European Union Council (86/609/EU) and Portuguese laws for the use of laboratory animals. All animal protocols were performed under a 'Group-I' license from the Direcção-Geral de Veterinária, Ministério da Agricultura, do Desenvolvimento Rural e das Pescas, Portugal.

Tissue collection, blood and intestinal fluid analysis

After 30 days of acclimation to the altered salinity, fish were captured and anesthetized in 2-phenoxyethanol (1:5000 vol/vol; Sigma-Aldrich, St Louis, MO, USA). Blood samples were collected from the severed caudal peduncle into heparinized glass capillaries. Plasma was obtained by centrifugation (3500 ***g***, 5 min) and stored at −20°C until analysis. Fish were killed by decapitation and the whole intestine isolated. The intestinal fluid of individual fish was collected from the excised intestinal tract clamped (from pyloric caeca to anal sphincter) with two mosquito forceps, emptied into pre-weighed vials and centrifuged (12,000 ***g***, 5 min) to separate fluid from precipitate. The fluid was transferred to pre-weighed vials and the volume was measured to the nearest 0.1 µl (0.1 mg, assuming a density of 1). Precipitates, which include both organic (mucus) and inorganic carbonates, were dried at 50°C overnight and weighed to the nearest 0.1 mg. The results were normalized for fish mass and are presented as µl g^{-1} M_b or µg g^{-1} M_b. Intestinal samples were collected from individual fish, stored in RNA Later at 4°C (Sigma-Aldrich) until utilized for RNA extraction within 2 weeks. Tissue from two sections of intestine was collected: (1) the anterior intestine, corresponding to 3–4 cm caudal to the point of insertion of the pyloric caeca; and (2) the rectum, which corresponds to a section of distal intestine, 2–3 cm in length, delimited by the anal and the posterior/rectal sphincters.

Osmolality of plasma and intestinal luminal fluid was measured in 10 µl samples with a Vapro 5520 osmometer (Wescor, South Logan, UT, USA). Intestinal fluid titratable alkalinity (HCO_3^- + CO_3^{2-}) was manually measured with the double titration method using a combination semi-micro pH electrode (HI1330B, Hanna Instruments, Smithfield, RI, USA) attached to a pH meter (PHM84, Radiometer, Copenhagen, Denmark): 50 µl of the intestinal fluid samples was diluted in 10 ml NaCl (40 mmol l^{-1}), gassed with CO_2-free gas for 30 min to remove CO_2 and titrated to pH 3.8 with 10 mmol l^{-1} HCl; an additional gassing period of 20 min was applied to remove any remaining CO_2 and the sample was back titrated to its original pH with 10 mmol l^{-1} NaOH. The volume difference between added acid and base in both titrations and titrant molarities was used to calculate total HCO_3^- equivalents (mequiv l^{-1}).

Gravimetric water absorption

Intestinal water absorption in sea bream gut sacs was measured following methods previously described (Grosell and Taylor, 2007; Scott et al., 2008) in symmetric conditions. The abdominal regions were exposed and the whole intestinal tract removed to a Petri dish containing pre-gassed (0.3% CO_2 + 99.7% O_2) serosal solution (160 mmol l^{-1} NaCl, 1 mmol l^{-1} $MgSO_4$, 2 mmol l^{-1} NaH_2PO_4, 1.5 mmol l^{-1} $CaCl_2$, 5 mmol l^{-1} $NaHCO_3$, 3 mmol l^{-1} KCl, 5.5 mmol l^{-1} glucose and 5 mmol l^{-1} Hepes, pH 7.800). The lumen was flushed and cleaned, and the anterior intestine and rectum isolated. Intestinal sacs were prepared by sealing one of the edges with a Teflon tape ligature and filled with 0.8 ml (anterior intestine) or 0.15 ml (rectum) of physiological saline (symmetric conditions, serosal solution). Once filled, care was taken to remove gas bubbles and a second

ligature was applied to create a watertight preparation with an internal pressure of 15 cm of water in PE50 polythene tubing. The sacs were rested for 30–40 min in physiological solution with gassing (0.3% CO_2 + 99.7% O_2). For calculation of water absorption, the intestinal sacs were weighed (to the nearest 0.1 mg) at 10 min intervals over 1 h. At the end of the experimental period, the sacs were opened, flattened and overlaid on millimetric paper to measure the surface area. Water absorption was expressed as $\mu l\,h^{-1}\,cm^{-2}$.

Intestinal HCO_3^- secretion

A segment of anterior intestine and rectum was excised, mounted on tissue holders (P2413, 0.71 cm^2, Physiologic Instruments, San Diego, CA, USA) and positioned between two half-chambers (P2400, Physiologic Instruments) containing 1.5 ml of serosal and apical saline. The composition of these saline solutions that simulated *in vivo* conditions for the sea bream (Fuentes et al., 2006) was as follows. Serosal saline: 160 mmol l^{-1} NaCl, 1 mmol l^{-1} $MgSO_4$, 2 mmol l^{-1} NaH_2PO_4, 1.5 mmol l^{-1} $CaCl_2$, 5 mmol l^{-1} $NaHCO_3$, 3 mmol l^{-1} KCl, 5.5 mmol l^{-1} glucose and 5 mmol l^{-1} Hepes, pH 7.800, gassed with 0.3% CO_2 + 99.7% O_2. Apical saline: 88 mmol l^{-1} NaCl, 9.5 mmol l^{-1} $MgCl_2$, 3 mmol l^{-1} KCl, 7.5 mmol l^{-1} $CaCl_2$, 126.5 mmol l^{-1} $MgSO_4$ and 1 mmol l^{-1} Na_2HPO4, gassed with 100% O_2 and pH maintained at 7.800 throughout the experiments by pH-Stat (see below). The temperature was maintained at 22°C throughout all experiments. All bioelectrical variables were monitored by means of Ag/AgCl electrodes (with tip asymmetry <1 mV) connected to either side of the Ussing chamber with 3 mm-bore agar bridges (1 mol l^{-1} KCl in 3% agar). Transepithelial electrical potential (TEP, mV) was monitored by clamping of epithelia to 0 $\mu A\,cm^{-2}$. Epithelial conductance (G_t, $mS\,cm^{-2}$) was manually calculated (Ohm's law) using the voltage deflections induced by a 10 $\mu A\,cm^{-2}$ bilateral pulse of 2 s every minute. Current injections were performed by means of a VCC 600 amplifier (Physiologic Instruments). For pH-Stat control, a pH electrode (PHC 4000-8, Radiometer) and a microburette tip were immersed in the luminal saline and connected to a pH-Stat system (TIM 854, Radiometer). To allow pulsing (for G_t calculation) during pH measurements, the amplifier was grounded to the titration unit. The configuration of amplifier/pH-Stat system used in this study is similar to that first established for the characterization of HCO_3^- secretion in the intestine of the Gulf toadfish (Grosell and Genz, 2006; Guffey et al., 2011; Taylor et al., 2010) and provides rates of intestinal secretion similar to those obtained by the double titration method in the intestine of the sea bream (Fuentes et al., 2010b).

Measurement of HCO_3^- secretion was performed on luminal salines at physiological pH 7.800 during all experiments. The volume of the acid titrant (2.5 mmol l^{-1} HCl) was recorded and the amount of HCO_3^- secreted (nmol $h^{-1}\,cm^{-2}$) was calculated from the volume of titrant added, the concentration of the titrant and the surface area (cm^2). All experiments comprised 1 h of tissue stable voltage and HCO_3^- secretion.

Short-circuit current measurement

The anterior intestine and rectum were collected, isolated and mounted as previously described (Fuentes et al., 2010b) on a tissue holder of 0.71 cm^2 and positioned between two half-chambers containing 2 ml of serosal physiological saline (see above). During the experiments the tissue was bilaterally gassed with 0.3% CO_2 + 99.7% O_2 and the temperature was maintained at 22°C. Short-circuit current (I_{sc}, $\mu A\,cm^{-2}$) was monitored by clamping the epithelia to 0 mV. Epithelial conductance (G_t, $mS\,cm^{-2}$) was manually calculated (Ohm's law) using the current deflections induced by a 2 mV pulse of 3 s every minute. Voltage clamping and current injections were performed by means of a DVC-1000 voltage clamp amplifier (WPI, Sarasota, FL, USA) or a VCCMC2 voltage/current clamp (Physiologic Instruments). Bioelectrical parameters for each tissue were recorded after the tissue achieved a steady state, usually between 30 and 40 min after mounting.

qPCR

RNA extraction, cDNA synthesis and cloning

Total RNA was extracted using Total RNA Kit I (E.Z.N.A, Omega Bio-tek, Norcross, GA, USA) following the manufacturer's instructions, and the quantity and quality assessed (Nanodrop 1000, Thermo Scientific, Waltham, MA, USA). Prior to cDNA synthesis, RNA was treated with DNase using a DNA-free kit (Ambion, Austin, TX, USA) following the supplier's instructions. Reverse transcription of RNA was carried out in a final reaction volume of 20 µl using 0.5 µg of DNase-treated RNA, 1 mmol l^{-1} of dNTPs, 1 µg of random hexamer primers [$pd(N)_6$, GE Healthcare, Munich, Germany] and 40 U of MMLV RT (Promega, Madison, WI, USA) in the presence of 25 U of RNAguard RNase inhibitor (GE Healthcare).

Primer design

cDNA sequences of the ion transporters of interest [*SLC26a6*, *SLC26a3*, *SLC4a4*, *Atp6v1b* (V-type proton pump β subunit), *NKCC1*, *NKCC2* and *CFTR*] were extracted from the EST collection

Table 1. Details of primers used for RT-PCR

Gene	Primer	Sequence (5′ to 3′)	T_a (°C)	Product size (bp)	NCBI accession no.
NKCC1	Forward	TGCAGTGATGCTGCATGCGGATT	60	134	GU183823
	Reverse	CCGGCAGAGATGATGGGACCA			
NKCC2	Forward	ACGGAGTCCAAGAAAACCACGGG	60	143	FP335045
	Reverse	CCAGCCAGGATTCCGGTCGC			
CFTR	Forward	GGAGGGCCCGACCTCGTCAT	60	175	GU183822
	Reverse	CTGTTCGTCCCAGCAGGCCC			
SLC26a3	Forward	ATCTCGGCTCTGAAGGGACT	60	162	AM973894
	Reverse	GAGCATTTCTGTCCCTGCTC			
SLC26a6	Forward	GCGGGACTGTTCAGCGGAGG	60	176	FM155691.1
	Reverse	TGCGAACACGCCTGAACGGCA			
SLC4a4	Forward	ACCTTCATGCCACCGCAGGG	60	128	FM157528.1
	Reverse	CGCCGCCGCCGATAACTCTT			
Atp6v1b	Forward	TGTCTGCCTTTTCCTGAACC	60	180	FG266172.1
	Reverse	TGGGGATCTGGGTGATAGAG			

T_a, annealing temperature.

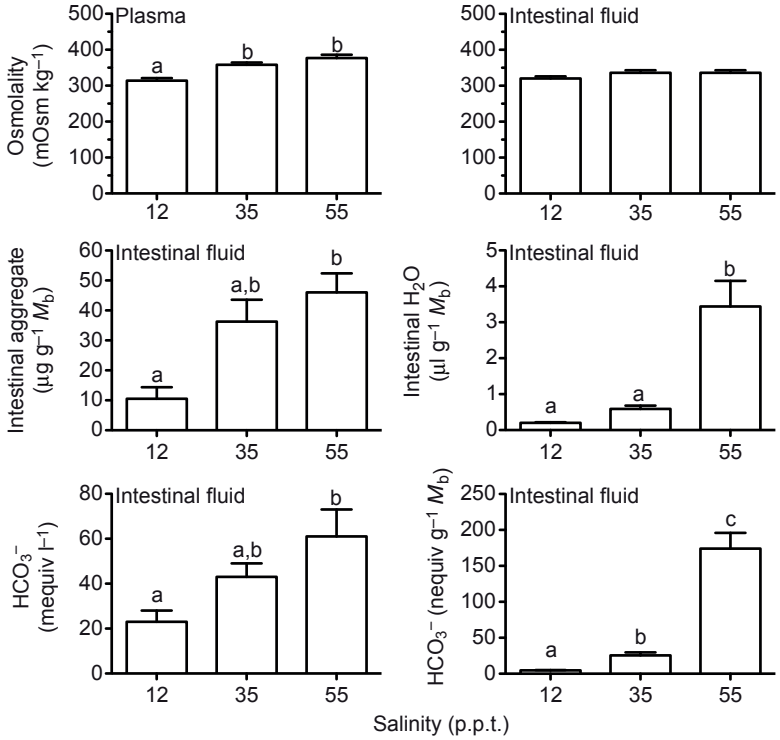

Fig. 1. Plasma and intestinal fluid osmolality, total aggregate content (M_b, body mass), total fluid content, intestinal fluid HCO_3^- and total HCO_3^- (normalized to fish M_b) in juvenile sea bream 30 days after transfer from 35 p.p.t. salinity to 12, 35 and 55 p.p.t. Each bar represents the mean + s.e.m. (N=5–10). Different lowercase letters indicate significant differences (P<0.05, one-way ANOVA, followed by the Bonferroni *post hoc* test).

database (dbEST) at the National Center of Biotechnology (NCBI, http://blast.ncbi.nlm.nih.gov/) using TBLASTn queries of known protein or deduced protein sequences from other fish species. Extracted sequences were compared by multisequence alignment using Clustal X to establish their identity (Larkin et al., 2007). Primer pairs were designed using the software Primer3 (http://frodo.wi.mit.edu/) running under the EBioX (http://www.ebioinformatics.org/) interface for Macintosh. Table 1 shows primer sequences, amplicon sizes and NCBI accession numbers of the target sequences.

Real-time qPCR amplifications were performed in duplicate in a final volume of 10 μl with 5 μl SsoFast EvaGreen Supermix (Bio-Rad, Hercules, CA, USA) as the reporter dye, 25 ng cDNA, and 0.3 pmol l^{-1} each of the forward and reverse primer. Amplifications were performed in 96-well plates using the One-step Plus sequence-detection system (Applied Biosystems, Foster City, CA, USA) with the following protocol: denaturation and enzyme activation step at 95°C for 2 min, followed by 40 cycles of 95°C for 5 s and 60°C for 10 s. After the amplification phase, a dissociation step was carried out at 95°C for 10 s, 60°C for 10 s, and 95°C for 10 s. For normalization of cDNA loading, all samples were run in parallel using 18S rRNA. To estimate efficiencies, a standard curve was generated for each primer pair from 10-fold serial dilutions (from 1 to 0.001 ng) of a pool of first-strand cDNA template from all samples. Standard curves represented the cycle threshold value as a function of the logarithm of the number of copies generated, defined arbitrarily as one copy for the most diluted standard. All calibration curves exhibited correlation coefficients R^2>0.98, and the corresponding real-time PCR efficiencies were >99%.

Immunohistochemistry

Immunohistochemical localization of CFTR, NKCC and NKA in sections of anterior intestine and rectum of sea bream acclimated to water of different salinity was performed as previously described (Wilson et al., 2007). Prior to primary antibody incubation, sections were pre-treated with 0.05% citraconic anhydride (pH 7.4) for 30 min at 100°C. Sections were incubated overnight at 4°C with mouse monoclonal hCFTR antibody c-term (1:400 dilution; R&D Systems, Minneapolis, MN, USA), and mouse monoclonal NKCC antibody (1:200) (Lytle et al., 1995) used in combination with the affinity-purified rabbit anti-NKA α-subunit antibody (1:500) (Wilson et al., 2007). The secondary antibodies used were goat anti-mouse Alexa Fluor 568 and goat anti-rabbit Alexa Fluor 488 (1:500; Invitrogen, Carlsbad, CA, USA). The sections were viewed on a Leica DM6000B wide-field epi-fluorescence microscope and images were captured using a digital camera (Leica DFC 340 FX, Lisbon, Portugal). Preliminary testing was conducted with single antibodies and with negative controls (peptide blocking, normal host sera and culture supernatant).

Statistical analysis

Data are expressed as means ± s.e.m. unless otherwise stated. Prior to statistical analysis, normality and homogeneity of variance were assessed. Differences in plasma osmolality, intestinal fluid osmolality, intestinal water content, intestinal aggregate content and intestinal HCO_3^- content were established by one-way ANOVA followed by the *post hoc* Bonferroni test. Differences in intestinal water absorption, HCO_3^- secretion, I_{sc}, tissue resistance and gene expression were analyzed by two-way ANOVA considering salinity (12, 35 and 55 p.p.t.) and intestinal region (anterior intestine and rectum) as the main effects. A significant interaction was interpreted by a subsequent simple-effects analysis with Bonferroni correction. All statistical analysis was performed with Prism 5.0 (GraphPad Software). Groups were considered significantly different at P<0.05.

RESULTS

Plasma and fluid analysis

The osmolality of sea bream plasma decreased significantly in fish transferred from 35 p.p.t. (control) to 12 p.p.t. (low salinity) but did

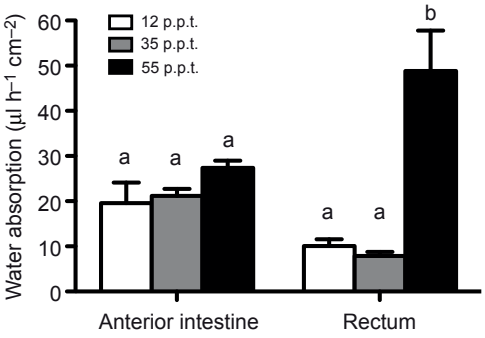

Fig. 2. Water absorption as measured in intestinal sacs prepared from the anterior intestine and the rectum of juvenile sea bream 30 days after transfer from 35 p.p.t. salinity to 12, 35 and 55 p.p.t. Each bar represents the mean + s.e.m. (N=4–6). For a given intestinal region, different lowercase letters indicate significant differences among salinities (P<0.05).

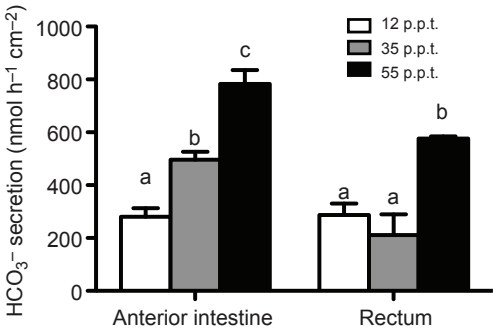

Fig. 3. HCO_3^- secretion as measured in Ussing chambers by pH-Stat in preparations from the anterior intestine and the rectum of juvenile sea bream 30 days after transfer from 35 p.p.t. salinity to 12, 35 and 55 p.p.t. Each bar represents the mean + s.e.m. (N=4–6). For a given intestinal region, different lowercase letters indicate significant differences among salinities (P<0.05).

not change when fish were transferred to 55 p.p.t. (high salinity). No effect of salinity on intestinal fluid osmolality was detected (Fig. 1).

The total intestinal dried aggregate (including mucus + carbonate aggregates) content in control fish was 35 µg g^{-1} M_b and significant differences were found only between extreme salinities (Fig. 1). However, the total intestinal fluid content at a given time was between 5- and 8-fold higher in animals at high salinity. HCO_3^- concentration in the intestinal fluid of control fish was around 40 mequiv l^{-1} (Fig. 1) and salinity transfer to high or low salinity resulted in a parallel increase or decrease, respectively, of HCO_3^-, which was only significantly different between low and high salinity. However, when concentrations were normalized to fluid volume content and fish M_b, the total HCO_3^- fluid content expressed as nequiv g^{-1} M_b was between 30 and 6 times higher in high salinity than in low salinity or control (Fig. 1).

Gravimetric water absorption

Basal values of water absorption in control fish were higher in the anterior intestine (22.1±1.90 µl cm^{-2} h^{-1}) than in the rectum (7.50±0.91 µl cm^{-2} h^{-1}, Fig. 2). No significant effect of salinity was observed on water absorption in the anterior intestine, while a 4- to 5-fold increase was observed in the rectum of fish at high salinity (Fig. 2).

HCO_3^- secretion and epithelial bioelectrical properties

HCO_3^- secretion in the anterior intestine of control fish was 495 nmol cm^{-2} h^{-1} and the rectum averaged a lower secretion of 211 nmol h^{-1} cm^{-2} (Fig. 3). In the anterior intestine, significantly lower (280 nmol cm^{-2} h^{-1}) or higher (783 nmol cm^{-2} h^{-1}) HCO_3^- secretion rates were observed in low or high salinity, respectively (Fig. 3). In the rectum, a reduction in salinity resulted in an unchanged HCO_3^- secretion, while an increase in salinity resulted in a significant 3- to 4-fold increase in HCO_3^- secretion (Fig. 3).

The I_{sc} of intestinal regions of the sea bream in response to salinity is shown in Fig. 4. Positive I_{sc} values indicate secretory currents; absorptive currents are shown by negative values. Mean values of I_{sc} in the anterior intestine and rectum of the sea bream after long-term adaptation are dependent on salinity and intestinal region. In control and high salinity fish, the anterior intestine showed a small but consistent absorptive current, while in low salinity fish a secretory current was observed. In contrast, the rectum of all fish showed a secretory/positive current, which was significantly higher at high salinity (Fig. 4).

G_t in the anterior intestine was between 10 and 15 mS cm^{-2}, regardless of the external salinity, while in the rectum high salinity fish had significantly lower G_t values.

qPCR

Changes in *Atp6v1b* expression are shown in Fig. 5. Regardless of the external salinity, *Atp6v1b* expression was lower in the anterior intestine than in the rectum. In the anterior intestine, *Atp6v1b* expression was higher at high salinity, while in the rectum expression levels were significantly lower in low salinity fish (Fig. 5).

Fig. 5 also shows the expression of *SLC4a4*, which was on average 5- to 7-fold higher in the anterior intestine than in the rectum depending on the external salinity. No changes in expression were observed in the rectum of fish acclimated long-

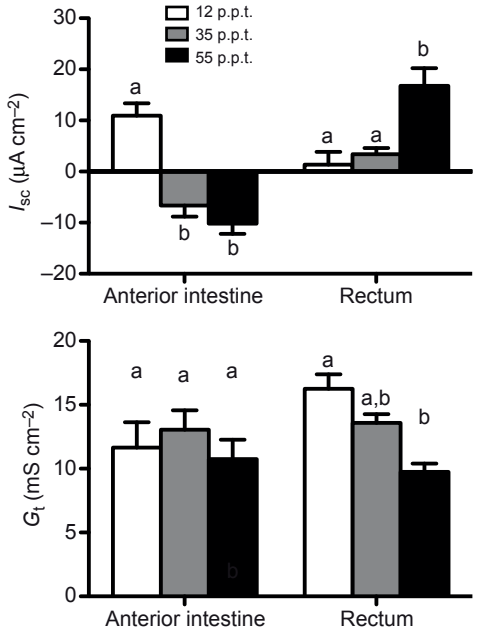

Fig. 4. Short-circuit current (I_{sc}) and tissue conductance (G_t) in the anterior intestine and the rectum of juvenile sea bream 30 days after transfer from 35 p.p.t. salinity to 12, 35 and 55 p.p.t. Each bar represents the mean + s.e.m. (N=6–7). For a given intestinal region, different lowercase letters indicate significant differences among salinities (P<0.05).

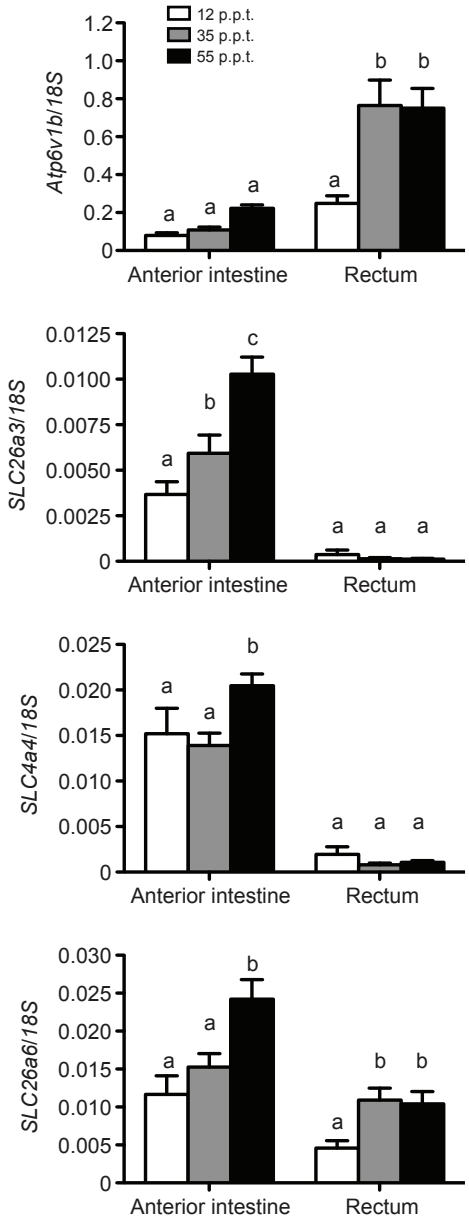

Fig. 5. Relative expression (ratio of gene of interest:*18S*) of *Atp6v1b*, *SLC26a3*, *SLC4a4* and *SLC26a6* in the anterior intestine and the rectum of juvenile sea bream 30 days after transfer from 35 p.p.t. salinity to 12, 35 and 55 p.p.t. Each bar represents the mean + s.e.m. (*N*=6–7). For a given intestinal region, different lowercase letters indicate significant differences among salinities (P<0.05).

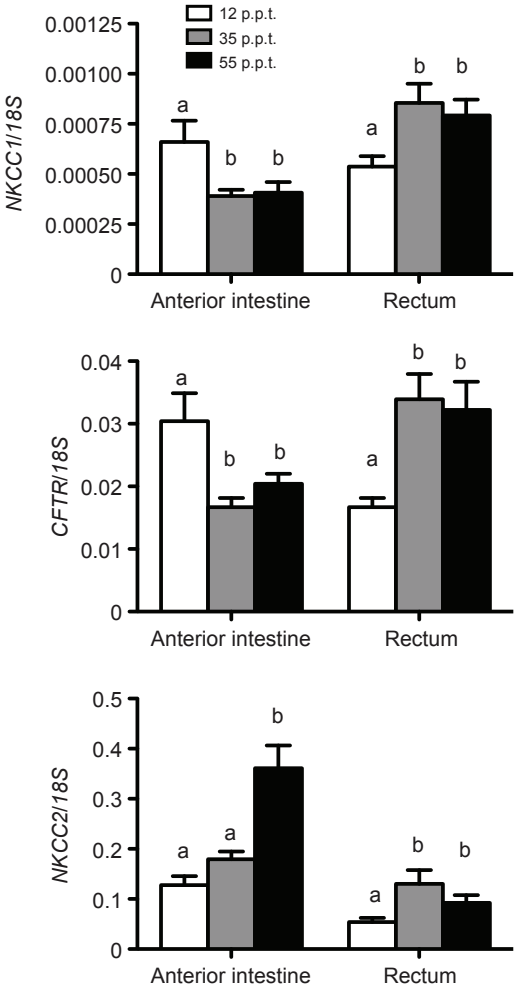

Fig. 6. Relative expression (ratio of gene of interest:*18S*) of *NKCC1*, *CFTR* and *NKCC2* in the anterior intestine and the rectum of juvenile sea bream 30 days after transfer from 35 p.p.t. salinity to 12, 35 and 55 p.p.t. Each bar represents the mean + s.e.m. (*N*=6–7). For a given intestinal region, different lowercase letters indicate significant differences among salinities (P<0.05).

term to either salinity. However, a significant increase in expression was observed in the anterior intestine at high salinity (Fig. 5).

A similar regionalization was observed in the expression of *SLC26a3*, with severalfold higher expression in the anterior intestine than in the rectum at all salinities. In the anterior intestine, *SLC26a3* showed significantly different levels of expression that parallel the external salinity (Fig. 5), while no effects of salinity were observed in the rectum.

Expression of *SLC26a6* was observed in the anterior intestine and the rectum of the sea bream at all salinities. Independent significant effects of salinity and intestinal region were observed. Higher levels of *SLC26a6* expression were found in the anterior intestine at high salinity, while in the rectum significantly lower expression levels were observed in low salinity (Fig. 5).

Fig. 6 shows mean expression of *NKCC1* in the anterior intestine and the rectum of salinity-challenged sea bream. Significantly higher levels of expression of *NKCC1* were observed at low salinity in the anterior intestine. In contrast, expression levels in the rectum were significantly lower at low salinity (Fig. 6).

CFTR expression (Fig. 6) exhibited a similar pattern to that of *NKCC1*, with higher levels of expression of *CFTR* at low salinity in the anterior intestine and lower expression levels in the rectum in low salinity fish (Fig. 6).

NKCC2 expression was observed in the anterior intestine and the rectum of sea bream at all salinities. In the anterior intestine, high salinity fish showed significantly higher levels of *NKCC2* expression than fish in the other groups. In contrast, expression levels of *NKCC2* in the rectum of fish challenged with low salinity were significantly lower (Fig. 6).

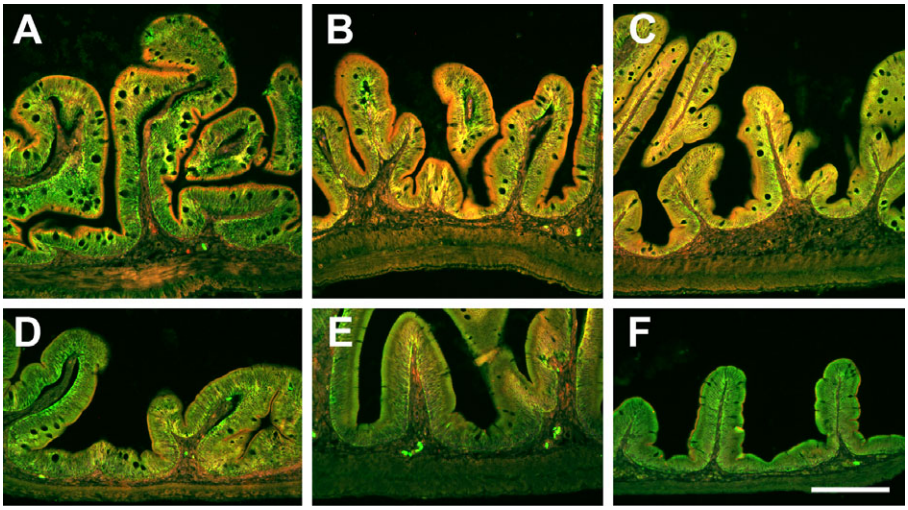

Fig. 7. Immunofluorescence localization of CFTR (red) and Na^+/K^+-ATPase (green) in the anterior intestine (A–C) and the rectum (D–F) of sea bream 30 days after transfer from 35 p.p.t. salinity to 12 p.p.t. (A,D), 35 p.p.t. (B,E) and 55 p.p.t. (C,F). Sections were counterstained with nuclear stain DAPI (4′,6-diamidino-2-phenylindole; blue) and overlaid with the DIC (differential interference contrast) image for tissue orientation. Scale bar, 250 μm.

Immunohistochemistry

Apical CFTR staining of brush border columnar epithelial cells was only apparent in the rectum of high salinity fish (Fig. 7F), while in the apical region of the anterior intestinal epithelium it had a diffuse staining pattern. Strong apical NKCC staining of brush border columnar epithelial cells of both anterior intestine and rectum was observed (Fig. 8), which appeared to be stronger in the high salinity fish. Both NKCC and CFTR labeling strength appeared to positively correlate with salinity. Na^+/K^+-ATPase α-subunit immunoreactivity was detected in the basolateral membrane of epithelial cells in both the intestine and rectum. Strong Na^+/K^+-ATPase immunoreactivity was also detected in isolated cells in the lamina propria (Figs 7, 8).

DISCUSSION

The sea bream are unable to withstand freshwater (Fuentes et al., 2010a). However, when challenged with external salinities in the range 5–60 p.p.t. they are able to adjust salinity-driven gill and plasma changes within 3 weeks of transfer (Laiz-Carrion et al., 2005). In consequence, the results of this study are steady-state patterns of fish fully adapted to different environmental salinities.

Intestinal water absorption

Following methods previously detailed (Grosell and Taylor, 2007; Scott et al., 2008), water absorption in gut sacs was measured under symmetric conditions to avoid passive water absorption driven by osmotic gradients. Measurement of water absorption in symmetric conditions, as opposed to *in vivo* like (asymmetric) saline, may provide an overestimate of water absorption as shown for the Gulf toadfish (Genz et al., 2011; Grosell and Taylor, 2007). The sea bream intestinal fluid osmolality remains unchanged (Fig. 1) after long-term challenge with low/high salinity and the use of the same saline provides a valid basis for comparison of the potential water absorption in different intestinal regions and the effect of salinity. Under these experimental conditions, the values of water absorption obtained along the sea bream intestine are in keeping with those described for other marine species such as the killifish, *Fundulus heteroclitus* (Scott et al., 2008; Wood and Grosell, 2012), the Japanese eel (Aoki et al., 2003) or the Gulf toadfish (Grosell and Taylor, 2007).

Like other marine fish (Fuentes and Eddy, 1997b) the sea bream drink high amounts of seawater, at a rate of around 5 $ml\,h^{-1}\,kg^{-1}$ (Guerreiro et al., 2002), and the whole intestine is preferentially

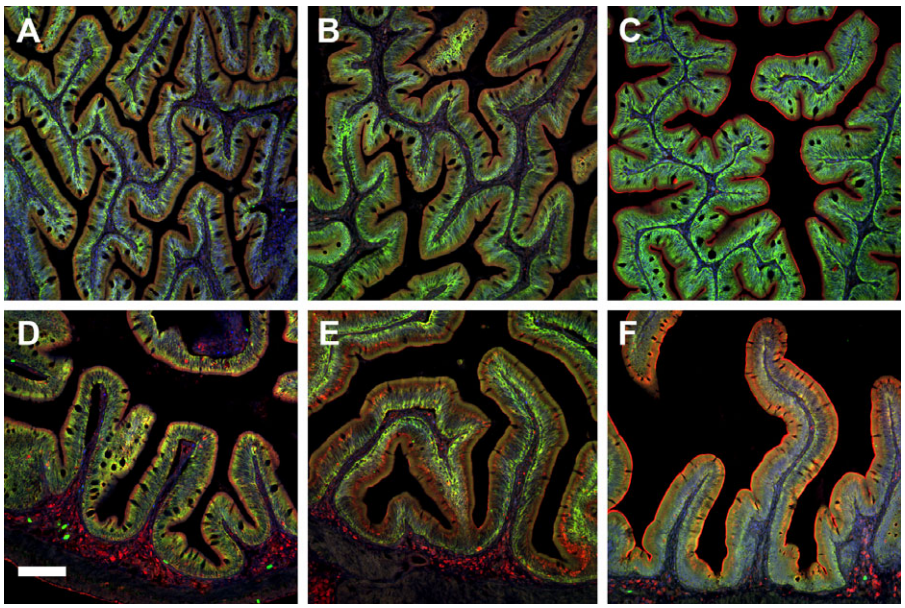

Fig. 8. NKCC-like (red) immunoreactivity and Na^+/K^+-ATPase (green) in the anterior intestine (A–C) and the rectum (D–F) of sea bream 30 days after transfer from 35 p.p.t. salinity to 12 p.p.t. (A,D), 35 p.p.t. (B,E) and 55 p.p.t. (C,F). Sections were counterstained with nuclear stain DAPI (blue) and overlaid with the DIC image for tissue orientation. Scale bar, 100 μm.

absorptive in relation to water. However, specific rates vary along the intestinal tract and higher water absorption was observed in the anterior intestine than in the rectum of control fish. High and low salinity have little effect on water absorption in the anterior intestine, which averaged 20–25 $\mu l\,h^{-1}\,cm^{-2}$ in fish adapted to 12, 35 or 55 p.p.t. These results are in agreement with the effects of salinity adaptation in the eel (Aoki et al., 2003) with a minor effect of salinity on water absorption in the anterior intestine. However, they contrast with the reduction of water absorption observed in killifish adapted to seawater when compared with brackish water (10% seawater)-adapted animals (Scott et al., 2008).

Water absorption in the rectum of the sea bream is highly salinity dependent and while adaptation to low salinity was without effect, the rectum of high salinity fish absorbs water at a rate about 5- to 8-times higher than control fish. This observation is in good agreement with the response of the posterior intestine of Japanese eels to salinity (Aoki et al., 2003), although the effect of high salinity in eels is less pronounced than in the sea bream.

These differences in response to salinity between the anterior intestine and the rectum are likely to reflect a difference in functional plasticity to salinity challenge in the two regions. The increase in salt load at high salinity is not reflected by an increase of osmolality in the plasma. In addition, regardless of the external salinity (12, 35 or 55 p.p.t.), the intestinal fluid has an unchanged osmolality of 320–330 $mOsm\,kg^{-1}$. This may be the result of both the altered drinking rates, as previously shown in salinity-challenged sea bream larvae (Guerreiro et al., 2004), and/or the adjustment of water absorption rates. In light of the water absorption data, we suggest that the plasticity of the rectum, likely in combination with increased drinking, enables the absorption of additional water that is necessary to sustain the plasma osmolality within narrow limits.

Intestinal HCO_3^- content and secretion

The levels of HCO_3^- observed in the intestinal fluid of the sea bream are ~40 $mequiv\,l^{-1}$, within the range described for a wide array of other marine species (Wilson et al., 2002). On a concentration basis, long-term exposure of sea bream to higher or lower external salinity results in a small parallel increase or decrease in HCO_3^- concentration, respectively. In addition to changes in HCO_3^- concentration in the fluid, we observed that the volume of fluid itself in the intestine of salinity-adapted sea bream is substantially different, and parallels external salinity (Fig. 1). Consequently, when the volume of intestinal fluid is considered and the total amount of HCO_3^- present in the fluid is calculated for a given time and normalized by fish mass, adaption to high salinity results in a 5- to 7-fold increase of fluid HCO_3^- content in the intestinal lumen (Fig. 1). The aggregate fraction measured in this study provides only a rough estimate of mineral content in the form of carbonates, as it might include a varying proportion of organic fraction at different salinities. However, the amount of intestinal precipitates remains unchanged (when compared with control fish), whilst water calcium concentration is 50% higher. A parallel observation was described *in vivo* in total HCO_3^- output (fluid + solid) in rectal fluid in the Gulf toadfish (Genz et al., 2008). Our interpretation of these observations is that fluid transit induced by drinking in fish at high salinity is greatly increased – an idea also supported by the substantial increase of total fluid present in the intestine of the sea bream at a given time. However, the increase in drinking seems to override the capacity of the intestine for aggregate precipitation. The high amount of HCO_3^- present in the intestinal fluid may be titrated by the action of a proton pump in the distal intestine to enhance rectal water absorption.

In keeping with the demonstration of HCO_3^- secretion in different regions of the intestine in the European flounder, Pacific Sanddab and lemon sole (Wilson et al., 2002), HCO_3^- secretion takes place in the anterior intestine and the rectum of the sea bream, although the anterior intestine secretes about twice as much HCO_3^- as the rectum. HCO_3^- secretion rates in the sea bream intestine measured by pH-Stat are within the range of those described in different intestinal sections of the Gulf toadfish and seawater-adapted trout (0.2–0.6 $\mu mol\,h^{-1}\,cm^{-2}$) (Grosell et al., 2009a; Guffey et al., 2011). In addition, higher secretion rates were observed at higher salinities both in the anterior intestine and in the rectum. In keeping with the heterogeneous effect of salinity on water absorption, there is a region-dependent effect in the capacity of the epithelium to secrete HCO_3^- in the intestine of the sea bream. Thus, the increase of HCO_3^- secretion in the rectum at high salinity is about 3-fold higher than the rate of control fish. However, it falls short of the 5- to 7-fold increase in water absorption observed in the same animals in the rectum. These results imply a strong relationship between water absorption and HCO_3^- secretion. However, while HCO_3^- secretion in the intestine is an important driving force for Cl^- *via* apical anion exchangers and subsequently water absorption (Grosell et al., 2005), the apical NKCC has an important role.

Molecular response to salinity

SLC4A4 (NBCe1) is an electrogenic Na^+-coupled HCO_3^- transporter that moves both ions into the cell (Romero et al., 2004). In fish intestine, SLC4a4 is located in the basolateral membrane of the enterocyte, is expressed at higher levels in seawater fish (Kurita et al., 2008) and is believed to constitute a bottleneck for the epithelial capacity of HCO_3^- secretion (Taylor et al., 2010). In keeping with a previous report in the intestine of the Gulf toadfish (Taylor et al., 2010), salinity-dependent higher expression of *SLC4a4* was observed in the anterior intestine of the sea bream. However, the levels of gene expression are compatible with a wide variation of HCO_3^- secretion in salinity-adapted fish (Fig. 3). It remains unknown whether this observation is related to stoichiometry transition of SLC4a4 in the sea bream. However, changes in the transport ratio of Na^+:HCO_3^- (1:2, 1:3, 1:4) have recently been demonstrated for the euryhaline pufferfish NBCe1 (Chang et al., 2012).

The SLC26 family of transporters as described in humans has a wide variety of members and epithelial transport functions. Different members carry SO_4^{2-} and oxalate, and operate as Cl^-/HCO_3^- exchangers or as selective Cl^- channels (Dorwart et al., 2008). Within this family, SLC26A3 and SLC26A6 are found in secretory epithelia and function as Cl^-/HCO_3^- exchangers (Ohana et al., 2009; Shcheynikov et al., 2006).

The intestinal HCO_3^- secretion in marine fish intestine relies on luminal Cl^-, which suggests a process mediated by apical Cl^-/HCO_3^- exchangers (Grosell et al., 2005; Wilson et al., 1996). Moreover, a study in mefugu (Kurita et al., 2008) has demonstrated a high HCO_3^- transport capacity of SLC26a6 in seawater fish intestine and differential expression as a function of salinity. In the sea bream intestine, both *SLC26a6* and *SLC26a3* are expressed, but at higher levels in the anterior intestine than in the rectum. An estimate based only on the expression data of both *SLC26a6* and *SLC26a3* (Fig. 5) and assuming linear relationships would predict a 2- to 3-fold higher HCO_3^- secretion in the anterior intestine of high salinity-adapted fish. This is in good agreement with the *in vitro* results of HCO_3^- secretion measured by pH-Stat (Fig. 3).

The rectum becomes more active at higher salinities and both water absorption and HCO_3^- secretion are enhanced. This increase is not substantiated by the expression data for either *SLC26a6* or

SLC26a3. In the rectum of high salinity fish and in line with expression levels of both *SLC26a6* and *SLC26a3*, no changes of water or HCO_3^- secretion could be predicted in relation to control fish. However, it is surprising that in both groups a high expression of *Atp6v1b* was observed, which is between 3- and 5-fold higher than in the anterior intestine. A previous study (Grosell et al., 2009b) has suggested that the electrogenic SLC26a6 is functionally linked to the activity of an electrogenic H^+-pump and regulated by its activity. In keeping with this idea, the high expression of *Atp6v1b* in the rectum of the sea bream at high salinity would predict a high activity of an apical H^+-pump in the rectum, resulting in high acid secretion. While carbonate aggregate formation and luminal acidification are supposedly opposing processes, independent activation of either would result in lower luminal osmolality to favor water absorption (Grosell et al., 2009b). The high water absorption observed in the rectum of high salinity fish is likely H^+-pump dependent. This would probably explain the comparatively lower than predicted intestinal aggregate presence observed in the intestine in high salinity fish, even when the total amount of HCO_3^- is 5- to 8-fold higher than in controls or low salinity fish, respectively. In light of the regional expression pattern of anion exchangers and the H^+-pump, and considering intestinal HCO_3^- and aggregate content in the lumen of high salinity fish, it seems clear that carbonate aggregate formation mediated by anion exchangers dominates in the anterior intestine. In turn, rectal acid secretion mediated by an apical H^+-pump titrates the high amounts of HCO_3^- to lower luminal osmolality and makes more water available for absorption. A similar distribution of expression, enzyme activity and physiological function of a V-type H^+-ATPase (Guffey et al., 2011) and cytosolic carbonic anhydrase (Sattin et al., 2010) between the anterior and posterior intestine (not the rectum) has recently been proposed in the Gulf toadfish.

Under voltage clamp and with symmetric salines in the Ussing chamber, I_{sc} of epithelia is the electrical representation of net epithelial ion transport. In the anterior intestine of the sea bream, the fish adapted to low salinity show a highly variable secretory current in the voltage-clamp experiments in Ussing chambers. This could reflect the absolute increase in the expression of *NKCC1* and the *CFTR*, mechanisms that constitute the Cl^- secretory pathway in epithelia (Cutler and Cramb, 2001; Cutler and Cramb, 2002). In the rectum, a prevailing secretory function was observed in fish at all salinities, with higher secretion at higher salinity. This result is in keeping with the expression data, where matching increases of both *NKCC1* and the *CFTR* are detected, and inmunodetection clearly shows CFTR protein expression in the apical membrane of the enterocyte (Fig. 7). In mammalian models, a reciprocal regulatory interaction between SLC26a3 and SLC26a6 and CFTR has been demonstrated (Ko et al., 2004). The rectum of high salinity fish is a region preferentially absorptive of water as shown in the sac preparation experiments. However, it is preferentially secretory in relation to Cl^- as shown in the Ussing chamber experiments. Although it may appear counter-intuitive, enhanced Cl^- secretion may stimulate the function of SLC26a6 transporters to favor Cl^- recycling, and thus stimulate Cl^--dependent water absorption mediated either by SLC26a6 or by NKCC2, and possibly, though this is less likely, by SLC26a3 (because of its residual expression).

The role of NKCC2 in epithelia is absorptive or re-absorptive (in the loop of Henle of mammals) (Gamba, 2005). It appears that Cl^- uptake is responsible for the majority of water absorption in intestinal epithelia of marine fish and the importance of a bumetanide-sensitive mechanism mediated by NKCC apical co-transporters has been established (Loretz, 1995). In fish, the *NKCC2* gene is expressed in several tissues, although its distribution is not widespread. For instance, in the brackish medaka (*Oryzias dancena*), it is preferentially expressed in the intestine and the kidney (Kang et al., 2010). *NKCC2* expression has been demonstrated to be salinity dependent and in European eels (*Anguilla anguilla*), for example, its expression in the intestine in seawater is up to 7-fold higher than in freshwater (Kalujnaia et al., 2007). In our study in the sea bream, *NKCC2* was found to be expressed in both the anterior intestine and the rectum. Given the absorptive nature of NKCC2, it is unsurprising to find higher levels of expression in the anterior intestine than in the rectum. This coincides with the 3-fold lower water absorption rates observed in the rectum in relation to the anterior intestine in sac preparations of control fish. In the anterior intestine of the sea bream, the expression pattern of *NKCC2* parallels absolute rates of water absorption. However, in the rectum, similar expression levels of *NKCC2* are compatible with a 4- to 5-fold difference in water absorption between fish adapted to 35 and 55 p.p.t., an issue probably related to protein trafficking and apical insertion of functional proteins. Interestingly, NKCC staining was observed in the rectum of all fish (Fig. 8). However, while in controls the staining has both apical and sub-apical distribution, it is strongly concentrated in the apical membrane of the enterocyte at high salinity, indicating that by location and protein functionality, it is likely that NKCC2 sustains most of the Cl^- uptake to enhance water absorption observed in the rectum of these fish.

It seems that the intestinal distribution of specific molecular mechanisms related to the processing of intestinal fluid responds to a similar pattern of anterior–posterior distribution, but species-specific differences exist. Previous studies in the Gulf toadfish (Guffey et al., 2011; Sattin et al., 2010; Taylor et al., 2010) have demonstrated the relative importance of the distal intestine (not the rectum) in osmoregulation in marine fish, with actions likely mediated by cytosolic carbonic anhydrase and a V-type proton pump. In the sea bream, we have described adaptive heterogeneous responses in different gastrointestinal sections that also indicate functional and partly exclusive physiological roles. Higher rates of epithelial HCO_3^- secretion that parallel external salinity are observed in the anterior intestine. Fish challenged with high salinities have much a higher fluid content of HCO_3^- equivalents, but not proportionally higher intestinal precipitates than control fish. It seems that carbonate precipitation is limited, likely by calcium availability. However, the rectum probably exploits this limitation. A V-type proton pump, highly expressed in the rectum, probably titrates the excess HCO_3^- to allow the observed increase of water absorption, mediated by Cl^--driven mechanisms, i.e. anion exchangers and/or NKCC.

ACKNOWLEDGEMENTS

We would like to thank the reviewers for their invaluable contribution to the manuscript.

FUNDING

This work was supported by the Portuguese Foundation for Science and Technology (Ministry of Science and Higher Education, Portugal and European Social Funds) grant [PTDC/MAR/104008/2008] to J.F.

REFERENCES

Aoki, M., Kaneko, T., Katoh, F., Hasegawa, S., Tsutsui, N. and Aida, K. (2003). Intestinal water absorption through aquaporin 1 expressed in the apical membrane of mucosal epithelial cells in seawater-adapted Japanese eel. *J. Exp. Biol.* **206**, 3495-3505.

Chang, M. H., Plata, C., Kurita, Y., Kato, A., Hirose, S. and Romero, M. F. (2012). Euryhaline pufferfish NBCe1 differs from nonmarine species NBCe1 physiology. *Am. J. Physiol. Cell Physiol.* **302**, C1083-C1095.

Cooper, C. A., Whittamore, J. M. and Wilson, R. W. (2010). Ca^{2+}-driven intestinal HCO_3^- secretion and $CaCO_3$ precipitation in the European flounder in vivo: influences on acid-base regulation and blood gas transport. *Am. J. Physiol. Regul. Integr. Comp. Physiol.* **298**, R870-R876.

Cutler, C. P. and Cramb, G. (2001). Molecular physiology of osmoregulation in eels and other teleosts: the role of transporter isoforms and gene duplication. *Comp. Biochem. Physiol.* **130A**, 551-564.

Cutler, C. P. and Cramb, G. (2002). Two isoforms of the $Na^+/K^+/2Cl^-$ cotransporter are expressed in the European eel (*Anguilla* anguilla). *Biochim. Biophys. Acta* **1566**, 92-103.

Dorwart, M. R., Shcheynikov, N., Yang, D. and Muallem, S. (2008). The solute carrier 26 family of proteins in epithelial ion transport. *Physiology (Bethesda)* **23**, 104-114.

Evans, D. H., Piermarini, P. M. and Choe, K. P. (2005). The multifunctional fish gill: dominant site of gas exchange, osmoregulation, acid-base regulation, and excretion of nitrogenous waste. *Physiol. Rev.* **85**, 97-177.

Faggio, C., Torre, A., Lando, G., Sabatino, G. and Trischitta, F. (2011). Carbonate precipitates and bicarbonate secretion in the intestine of sea bass, *Dicentrarchus labrax*. *J. Comp. Physiol. B* **181**, 517-525.

Fuentes, J. and Eddy, F. B. (1997a). Drinking in Atlantic salmon presmolts and smolts in response to growth hormone and salinity. *Comp. Biochem. Physiol.* **117A**, 487-491.

Fuentes, J. and Eddy, F. B. (1997b). Drinking in marine, euryhaline and freshwater teleost fish. In *Ionic Regulation in Animals* (ed. W. T. W. Potts, N. Hazon, F. B. Eddy and G. Flik), pp. 135-149. Berlin: Springer-Verlag.

Fuentes, J. and Eddy, F. B. (1997c). Effect of manipulation of the renin-angiotensin system in control of drinking in juvenile Atlantic salmon (*Salmo salar* L) in fresh water and after transfer to sea water. *J. Comp. Physiol. B* **167**, 438-443.

Fuentes, J., Soengas, J. L., Rey, P. and Rebolledo, E. (1997). Progressive transfer to seawater enhances intestinal and branchial Na^+-K^+-ATPase activity in non-anadromous rainbow trout. *Aquacult. Int.* **5**, 217-227.

Fuentes, J., Figueiredo, J., Power, D. M. and Canário, A. V. M. (2006). Parathyroid hormone-related protein regulates intestinal calcium transport in sea bream (*Sparus auratus*). *Am. J. Physiol. Regul. Integr. Comp. Physiol.* **291**, R1499-R1506.

Fuentes, J., Brinca, L., Guerreiro, P. M. and Power, D. M. (2010a). PRL and GH synthesis and release from the sea bream (*Sparus auratus* L.) pituitary gland in vitro in response to osmotic challenge. *Gen. Comp. Endocrinol.* **168**, 95-102.

Fuentes, J., Power, D. M. and Canário, A. V. M. (2010b). Parathyroid hormone-related protein-stanniocalcin antagonism in regulation of bicarbonate secretion and calcium precipitation in a marine fish intestine. *Am. J. Physiol. Regul. Integr. Comp. Physiol.* **299**, R150-R158.

Gamba, G. (2005). Molecular physiology and pathophysiology of electroneutral cation-chloride cotransporters. *Physiol. Rev.* **85**, 423-493.

Genz, J., Taylor, J. R. and Grosell, M. (2008). Effects of salinity on intestinal bicarbonate secretion and compensatory regulation of acid–base balance in *Opsanus beta*. *J. Exp. Biol.* **211**, 2327-2335.

Genz, J., McDonald, M. D. and Grosell, M. (2011). Concentration of $MgSO_4$ in the intestinal lumen of *Opsanus beta* limits osmoregulation in response to acute hypersalinity stress. *Am. J. Physiol. Regul. Integr. Comp. Physiol.* **300**, R895-R909.

Grosell, M. (2006). Intestinal anion exchange in marine fish osmoregulation. *J. Exp. Biol.* **209**, 2813-2827.

Grosell, M. (2011). Intestinal anion exchange in marine teleosts is involved in osmoregulation and contributes to the oceanic inorganic carbon cycle. *Acta Physiol. (Oxf.)* **202**, 421-434.

Grosell, M. and Genz, J. (2006). Ouabain-sensitive bicarbonate secretion and acid absorption by the marine teleost fish intestine play a role in osmoregulation. *Am. J. Physiol. Regul. Integr. Comp. Physiol.* **291**, R1145-R1156.

Grosell, M. and Taylor, J. R. (2007). Intestinal anion exchange in teleost water balance. *Comp. Biochem. Physiol.* **148A**, 14-22.

Grosell, M., Wood, C. M., Wilson, R. W., Bury, N. R., Hogstrand, C., Rankin, C. and Jensen, F. B. (2005). Bicarbonate secretion plays a role in chloride and water absorption of the European flounder intestine. *Am. J. Physiol. Regul. Integr. Comp. Physiol.* **288**, R936-R946.

Grosell, M., Genz, J., Taylor, J. R., Perry, S. F. and Gilmour, K. M. (2009a). The involvement of H^+-ATPase and carbonic anhydrase in intestinal HCO_3^- secretion in seawater-acclimated rainbow trout. *J. Exp. Biol.* **212**, 1940-1948.

Grosell, M., Mager, E. M., Williams, C. and Taylor, J. R. (2009b). High rates of HCO_3^- secretion and Cl^- absorption against adverse gradients in the marine teleost intestine: the involvement of an electrogenic anion exchanger and H^+-pump metabolon? *J. Exp. Biol.* **212**, 1684-1696.

Guerreiro, P. M., Fuentes, J., Canario, A. V. M. and Power, D. M. (2002). Calcium balance in sea bream (*Sparus aurata*): the effect of oestradiol-17beta. *J. Endocrinol.* **173**, 377-385.

Guerreiro, P. M., Fuentes, J., Flik, G., Rotllant, J., Power, D. M. and Canario, A. V. M. (2004). Water calcium concentration modifies whole-body calcium uptake in sea bream larvae during short-term adaptation to altered salinities. *J. Exp. Biol.* **207**, 645-653.

Guffey, S., Esbaugh, A. J. and Grosell, M. (2011). Regulation of apical H^+-ATPase activity and intestinal HCO_3^- secretion in marine fish osmoregulation. *Am. J. Physiol. Regul. Integr. Comp. Physiol.* **301**, R1682-R1691.

Hirano, T. and Mayer-Gostan, N. (1976). Eel esophagus as an osmoregulatory organ. *Proc. Natl. Acad. Sci. USA* **73**, 1348-1350.

Kalujnaia, S., McWilliam, I. S., Zaguinaiko, V. A., Feilen, A. L., Nicholson, J., Hazon, N., Cutler, C. P. and Cramb, G. (2007). Transcriptomic approach to the study of osmoregulation in the European eel *Anguilla anguilla*. *Physiol. Genomics* **31**, 385-401.

Kang, C. K., Tsai, H. J., Liu, C. C., Lee, T. H. and Hwang, P. P. (2010). Salinity-dependent expression of a Na^+, K^+, $2Cl^-$ cotransporter in gills of the brackish medaka *Oryzias dancena*: a molecular correlate for hyposmoregulatory endurance. *Comp. Biochem. Physiol.* **157A**, 7-18.

Kim, Y. K., Ideuchi, H., Watanabe, S., Park, S. I., Huh, M. and Kaneko, T. (2008). Rectal water absorption in seawater-adapted Japanese eel *Anguilla japonica*. *Comp. Biochem. Physiol.* **151A**, 533-541.

Ko, S. B., Zeng, W., Dorwart, M. R., Luo, X., Kim, K. H., Millen, L., Goto, H., Naruse, S., Soyombo, A., Thomas, P. J. et al. (2004). Gating of CFTR by the STAS domain of SLC26 transporters. *Nat. Cell Biol.* **6**, 343-350.

Kurita, Y., Nakada, T., Kato, A., Doi, H., Mistry, A. C., Chang, M. H., Romero, M. F. and Hirose, S. (2008). Identification of intestinal bicarbonate transporters involved in formation of carbonate precipitates to stimulate water absorption in marine teleost fish. *Am. J. Physiol. Regul. Integr. Comp. Physiol.* **294**, R1402-R1412.

Laiz-Carrion, R., Guerreiro, P. M., Fuentes, J., Canario, A. V. M., Del Rio, M. P. M. and Mancera, J. M. (2005). Branchial osmoregulatory response to salinity in the gilthead sea bream, *Sparus auratus*. *J. Exp. Zool. A Comp. Exp. Biol.* **303**, 563-576.

Larkin, M. A., Blackshields, G., Brown, N. P., Chenna, R., McGettigan, P. A., McWilliam, H., Valentin, F., Wallace, I. M., Wilm, A., Lopez, R. et al. (2007). Clustal W and Clustal X version 2.0. *Bioinformatics* **23**, 2947-2948.

Loretz, C. A. (1995). Electrophysiology of ion transport in teleost intestinal cells. In *Cellular and Molecular Approaches to Fish Ionic Regulation* (ed. C. M. Wood and T. J. Shuttleworth), pp. 25-56. San Diego, CA: Academic Press.

Lytle, C., Xu, J. C., Biemesderfer, D. and Forbush, B., 3rd (1995). Distribution and diversity of Na-K-Cl cotransport proteins: a study with monoclonal antibodies. *Am. J. Physiol.* **269**, C1496-C1505.

Musch, M. W., Orellana, S. A., Kimberg, L. S., Field, M., Halm, D. R., Krasny, E. J. J., Jr and Frizzell, R. A. (1982). Na^+-K^+-Cl^- co-transport in the intestine of a marine teleost. *Nature* **300**, 351-353.

Ohana, E., Yang, D. K., Shcheynikov, N. and Muallem, S. (2009). Diverse transport modes by the solute carrier 26 family of anion transporters. *J. Physiol.* **587**, 2179-2185.

Parmelee, J. T. and Renfro, J. L. (1983). Esophageal desalination of seawater in flounder: role of active sodium transport. *Am. J. Physiol.* **245**, R888-R893.

Romero, M. F., Fulton, C. M. and Boron, W. F. (2004). The SLC4 family of HCO_3^- transporters. *Pflugers Archiv.* **447**, 495-509.

Sattin, G., Mager, E. M., Beltramini, M. and Grosell, M. (2010). Cytosolic carbonic anhydrase in the Gulf toadfish is important for tolerance to hypersalinity. *Comp. Biochem. Physiol.* **156A**, 169-175.

Scott, G. R., Baker, D. W., Schulte, P. M. and Wood, C. M. (2008). Physiological and molecular mechanisms of osmoregulatory plasticity in killifish after seawater transfer. *J. Exp. Biol.* **211**, 2450-2459.

Shcheynikov, N., Wang, Y., Park, M., Ko, S. B., Dorwart, M., Naruse, S., Thomas, P. J. and Muallem, S. (2006). Coupling modes and stoichiometry of Cl^-/HCO_3^- exchange by slc26a3 and slc26a6. *J. Gen. Physiol.* **127**, 511-524.

Skadhauge, E. (1969). The mechanism of salt and water absorption in the intestine of the eel (*Anguilla anguilla*) adapted to waters of various salinities. *J. Physiol.* **204**, 135-158.

Taylor, J. R., Mager, E. M. and Grosell, M. (2010). Basolateral NBCe1 plays a rate-limiting role in transepithelial intestinal HCO3- secretion, contributing to marine fish osmoregulation. *J. Exp. Biol.* **213**, 459-468.

Whittamore, J. M., Cooper, C. A. and Wilson, R. W. (2010). HCO_3^- secretion and $CaCO_3$ precipitation play major roles in intestinal water absorption in marine teleost fish in vivo. *Am. J. Physiol. Regul. Integr. Comp. Physiol.* **298**, R877-R886.

Wilson, R., Gilmour, K., Henry, R. and Wood, C. (1996). Intestinal base excretion in the seawater-adapted rainbow trout: a role in acid–base balance? *J. Exp. Biol.* **199**, 2331-2343.

Wilson, R. W., Wilson, J. M. and Grosell, M. (2002). Intestinal bicarbonate secretion by marine teleost fish – why and how? *Biochim. Biophys. Acta* **1566**, 182-193.

Wilson, J. M., Leitao, A., Goncalves, A. F., Ferreira, C., Reis-Santos, P., Fonseca, A. V., da Silva, J. M., Antunes, J. C., Pereira-Wilson, C. and Coimbra, J. (2007). Modulation of branchial ion transport protein expression by salinity in glass eels (*Anguilla anguilla* L.). *Mar. Biol.* **151**, 1633-1645.

Wood, C. M. and Grosell, M. (2012). Independence of net water flux from paracellular permeability in the intestine of *Fundulus heteroclitus*, a euryhaline teleost. *J. Exp. Biol.* **215**, 508-517.